

Experimental study on flexural strength of modular composite profile beams

Hyung-Joon Ahn[†] and Soo-Hyun Ryu[‡]

Department of Architectural Engineering, Kon-Kuk University, Seoul, Korea

(Receive June 20, 2006, Accepted November 10, 2006)

Abstract. This study suggests modular composite profile beams, where the prefab concept is applied to existing composite profile beams. The prefab concept produces a beam of desired size having two types of profile: side module and bottom module. Module section will improve construction efforts because it offers several benefits : reduction of deflections due to creep and shrinkage, which might be found in existing composite profile beams; increase in span/depth ratio; and free prefabrication of any required beams. Based on the established analysis theory of composite profile beams, an analysis theory of modular composite profile beams was suggested, and analysis values were compared with experimental ones. The behavior of individual modules with increase of load was measured with a strain gauge, and the shear connection ratio between modules was analyzed by using the measured values. As a result of experiment, it was found that theoretical flexural strength on condition of full connection was 57%-80% by connection of modules for each specimen, and it is expected that flexural strength will approximate the theoretical levels through further module improvement.

Keywords: modular; composite profile; prefabrication; flexural strength.

1. Introduction

Studies on the use of reinforcing materials except for reinforcing bar have been continuously made in order to increase the strength and ductility of Reinforced concrete (RC) beam. Conventional methods cover reinforcement of a side plate onto an installed RC beam with bolt or adhesive bonding (Oehlers *et al.* 2000), or Fiber-Reinforced Polymer (FRP), (Minglan *et al.* 2004), Carbon Fiber Reinforced Plastics (CFRP), (Kim *et al.* 2004). On the contrary, reinforcing method using a profile sheet is advantageous in that it even considers constructional availability for use as a stay-in-place formwork addition to the merit of structural reinforcement together with reinforcing bar. Profile sheet has been first applied to slab, and studies of further applying this concept to beams have been made. As existing composite beams with profile sheet have been proven to be beneficial in terms of strength, stiffness, and serviceability limit state: they are available as permanent form of construction with the part of profile sheet; ductility, flexural strength, and shear strength are greatly improved; deflections due to creep and shrinkage are reduced; and span/depth ratio is 20% increased (Oehlers *et al.* 1994).

Flexural strength and shear strength between composite profile beam and reinforced concrete beam

[†]Professor

[‡]PhD Candidate, Corresponding author, E-mail: ryu129@hanmail.net

were compared by Oehlers *et al.* (1993), who also suggested a flexural strength equation based on the shear connection ratio and the rigid plastic analysis theory (1994). Uy *et al.* (1995) analyzed the load-deflection and moment-curvature characteristics of composite profile beam and a reinforced concrete beam, and compared them with those derived by use of a theoretical equation by using slip strain parameter. Also, they conducted numerical analysis of all the variables used in the theoretical equation (1995).

This study investigates the improvement of on-site applicability of the modular profile sheet which have convenience of construction ability. but have corrosion problem but protect corrosion by spread antirust paints or using Galvanized steel sheet. The modular profile sheet was divided into two types : side module profile sheet and bottom module profile sheet. Each module was connected with bolts to freely prefabricate the desired size of beams. The C-type and Lip-type modules are suggested. The specimens were arranged with variables of bolt connections and reinforcements of the tension reinforcing sheet. A proper module type was chosen between the two suggested module types. A shear connection level for various bolt connections was measured as suggested in the theoretical equation. The reinforcement efficiency of the tension sheet was examined. A strain gauge was attached to the side module to measure the neutral axis and the degree of module connections. The center deflection and local buckling of the profile sheet were also investigated. Local buckling behavior of profile, which was clarified by Oehlers *et al.* was applied to this study (1994).

2. Flexural strength

Flexural strength of C-type Modular Steel Concrete(MSC) beams was estimated by rigid plastic analysis, which applies the yielding strength to the shear section of the profile steel, and then $0.85 f_{ck}$ to the compression section of concrete by Oehlers' theoretical method, and the estimated theoretical value of bending moment was compared with the test result. Basic assumption applied to calculate the plastic moment was as follows :

Stress of $0.85 f_{ck}$ was equally distributed in the compression area of concrete, as shown in Fig. 1(c). The height of the compression area was calculated according to a ratio of the bond strength. The tensile strength of concrete is 0. In the profile steel, the yield strength (f_y) of compression on the top and the yield strength of tension on the bottom are equally distributed centered on the plastic neutral axis, and sectional form is simplified into an effective thickness (t_e) for theoretical analysis.

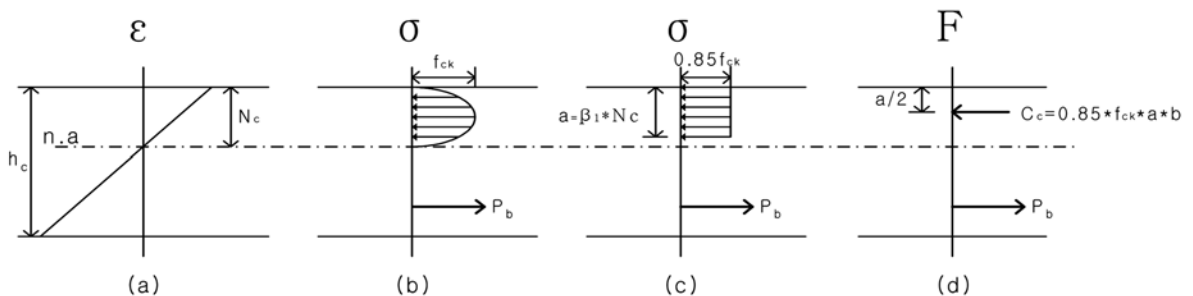


Fig. 1 Behavior of concrete element

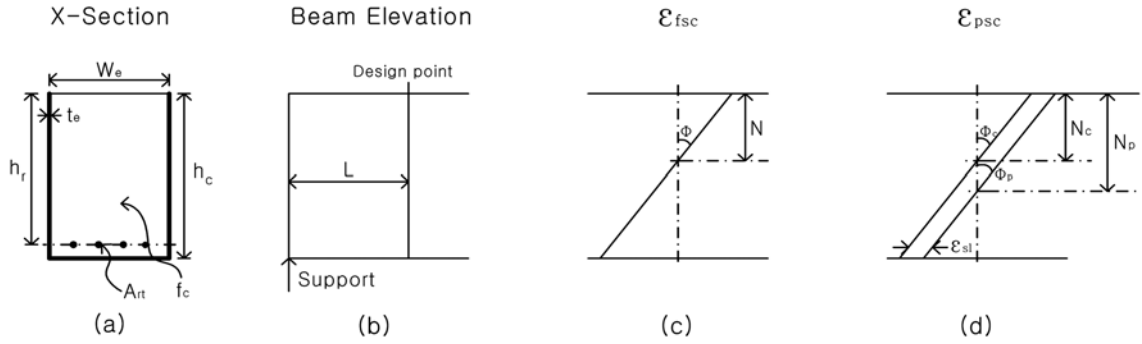


Fig. 2 Strain distribution in C-type MSC beam

2.1 Connection of individual modules with bolts

A section of C-type MSC beam is shown in Fig. 2(a). Fig. 2(c) and Fig. 2(d) show a strain curve as long as the concrete and profile steel go through full shear connection and partial shear connection, and neutral axis for concrete and profile steel. Connection is conceptualized in Fig. 2(b) : bond strength emerges and acts on the interface area(SL).

$$P_b = f_b SL \tag{1}$$

Here, P_b = maximum bond strength

f_b = Average shear bond strength steel profile/concrete interface

S = perimeter length of the interface between concrete and profile

L = distance L from the nearest edge of the profile sheet.

As the steel element and concrete go through full shear connection without slip, the steel element behaves consistently, as shown in Fig. 2(c). If the curvature ϕ and the bending moment are increased, the bond stress will increase, and if slip does not occur and reaches the maximum moment, the section will become fully composited. If the slip strain ϵ_{sl} occurs, as shown in Fig. 2(d), it goes through partial shear connection, and the flexural strength of the C-type MSC beam is decided in consideration of the strength distribution in each section element (steel element, concrete element).

Fig. 1 shows the behavior of the concrete element, neutral axis is indicated by N_c , and a indicates the depth of rectangular concrete compression stress block:

$$N_c = \frac{a}{\beta_1}$$

Here, $\beta_1 = 0.85 - 0.07(f_{ck} - 28)$.

If a concrete element is under bending strength and displays compression force, the concrete element and bond stress act as a compression element and tension element, respectively, and generate flexural strength. Then, considering force equilibrium, based on compression force and bond stress of concrete, tensile strength is indicated as follows:

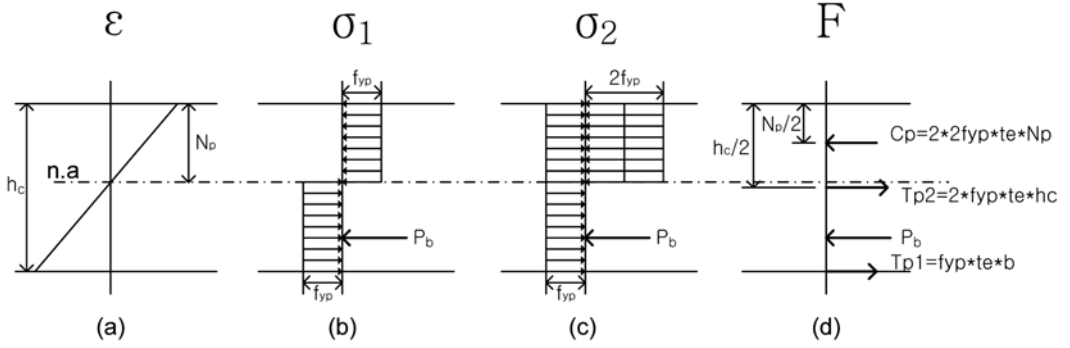


Fig. 3 Behavior of profile element

$$C_c = 0.85f_{ck}\beta_1N_c b = P_b \quad (2)$$

Here, C_c is the compressive force of concrete, and neutral axis N_c is defined:

$$N_c = \frac{P_b}{0.85f_{ck}\beta_1 b} \quad (3)$$

Fig. 3 shows the behavior of the steel element and N_p indicates the neutral axis. With respect to the general force equilibrium of concrete and profile steel, the bond stress acting on the tension part of the concrete shall act on the compression part of the steel element to establish force equilibrium. This force equilibrium is expressed by the following equation:

$$T_p = T_{p1} + T_{p2} = C_p + P_b \quad (4)$$

Here, T_p = tension force of steel sheet in the tension part
 T_{p1} = tension force of steel sheet in the bottom part
 T_{p2} = tension force of steel sheet in the side part
 C_p = compression force of steel sheet in the compression part.

Fig. 3(c) is a transformation of Fig. 3(b), where compressive stress f_y and tensile stress f_y are added to compression part of the profile steel, but there is no change in force equilibrium. If Eq. (4) is applied to the strength distribution strained as shown in Fig. 3(c),

$$f_y t_e (2h_c + b) = 2 \times 2f_y t_e N_p + P_b \quad (5)$$

If Eq. (5) is arranged in terms of N_p ,

$$N_p = \frac{f_y t_e (2h_c + b) - P_b}{4 f_y t_e} \quad (6)$$

The moment capacity of the C-type MSC beam is M_{ps} , and it may be obtained if section moment is taken

as shown in Fig. 2(d) and Fig. 3(d). As bond stress acts in the opposite direction and is positioned at the same position in the two sections, and its contribution to the moment is 0.

$$M_p = f_y t_e (h_c^2 + b h_c - 2N_p^2) - \frac{0.85 f_{ck} a^2 b}{2} \quad (7)$$

2.1.1 Full shear connection

For full shear connection, slip strain is 0, thus $N_c = N_p$. Therefore, bond stress $(P_b)_{fsc}$ to attain full shear connection is obtained by equipping Eq. (3) and Eq. (6):

$$(P_b)_{fsc} = \frac{f_y t_e (2h_c + b) \times 0.85 f_{ck} \beta_1 b}{4 f_y t_e + 0.85 f_{ck} \beta_1 b} \quad (8)$$

N_c and N_p are obtained by substitution of $(P_b)_{fsc}$ in Eq. (8) into Eq. (3) and Eq. (6), and it is substituted into Eq. (7), and then the bending moment (M_p) in full shear connection may be obtained.

2.1.2 Partial shear connection

N_c and N_p are obtained by transform of $(P_b)_{fsc}$ according to the degree of shear connection and then substituted into Eq. (7).

For example, if the shear connection is 50%,

$$(P_c)_{50\%} = 0.5 \times (P_b)_{fsc} \quad (9)$$

2.1.3 No shear connection

When $P_b = 0$, $N_c = 0$ in Eq. (3), and $N_p = \frac{f_y t_e (2h_c + b)}{4 f_y t_e}$ in Eq. (6). Then the concrete does not contribute to the flexural strength but just prevents the profile steel from buckling and displays only the moment caused by the profile steel.

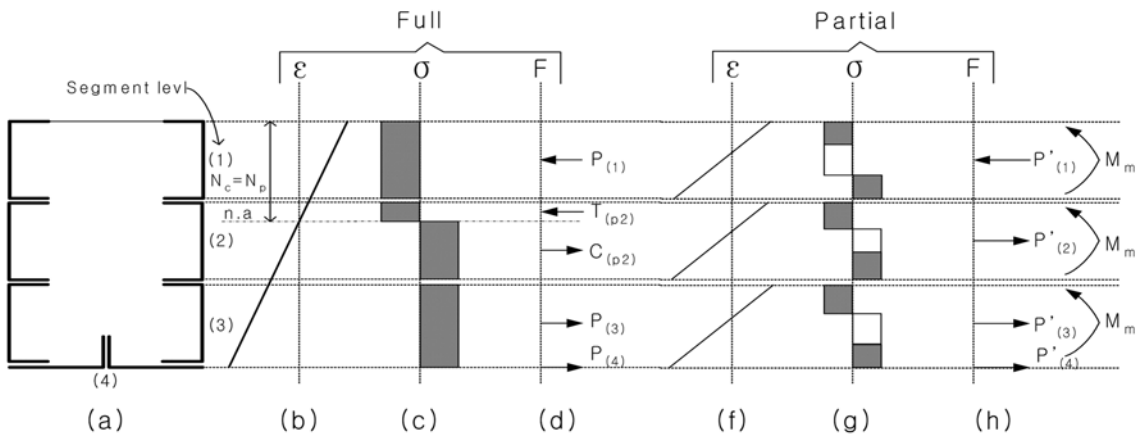


Fig. 4 Profile beam with shear connection

2.2 If individual modules are not connected with bolts

2.2.1 Full shear connection

If the concrete and profile steel of C-type MSC beam display full composite behavior by full shear connection, individual modules will show uniform behavior, as shown in Fig. 4(d). Then, the moment (M_p) is the same as the bending moment (M_p) in full shear connection, as described in Paragraph 2.1.

2.2.2 Partial shear connection

If the concrete and profile steel of C-type MSC beam are partially connected, individual modules do not display behavior in one form but partially separated, as shown in Fig. 4(g). Then, the moment (M_p) is obtained by addition of the moment from partial shear connection, moment of concrete, and moment of each steel plate.

$$(M_p)_{psc} = P'_{(4)} h_c + P'_{(3)} (h_c - 0.5h_m) + P'_{(2)} (h_c - 1.5h_m) - P'_{(1)} (h_c - 2.5h_m) - C_c \frac{a}{2} + 3M_m \quad (10)$$

Here, $P'_{(a)}$ = tension force of steel sheet in portion of not a slip

h_c = height of specimen

h_m = height of each module

M_m = bending moment of each module in portion of slip ratio

C_c = compression force of concrete in case of perfect shear connection.

2.2.3 No shear connection

If the concrete and profile steel of C-type MSC beam have no shear connection, $(M_p)_{msc}$ is the sum of moments of the modules. Then, the concrete does not contribute to strength, but just prevents the profile steel from buckling and displays only the moment cause by the profile steel.

3. Test setup

The specimen was loaded by two-point loading with a 490 kN test machine, as shown in Fig. 5 and Fig. 6. For measurement of deflection, two LVDTs were installed on both sides of the beam. The strain gauge? of

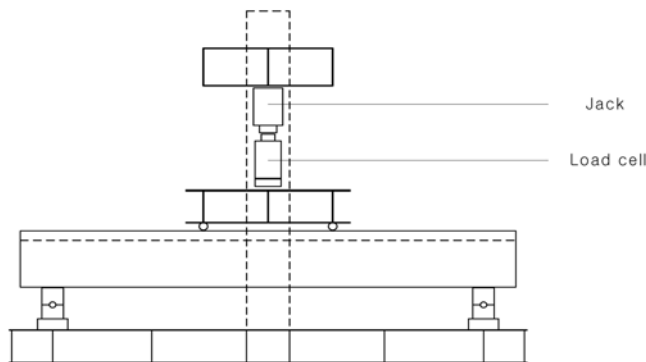


Fig. 5 Test setup

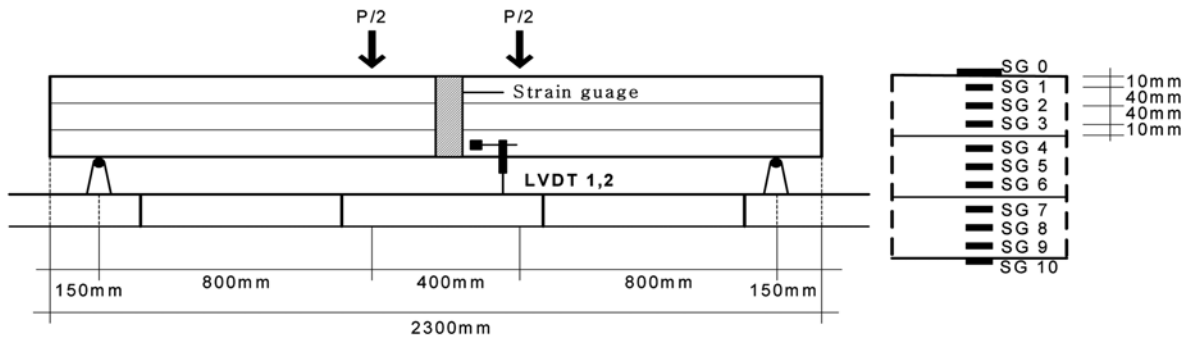


Fig. 6 Measure location

profile steel was attached to the top, middle and bottom of the side module and to the top and bottom of the beam. A concrete strain gauge was attached to the top of the center of the beam to observe the behavior of the concrete in compression.

4. Test specimens and material property

4.1 Test specimens

To test the flexural strength of the module section SC beam, six types of specimens suggested were made, as shown in Table 1. The thickness of the profile steel was 1.6 mm, beam width 200 mm, and beam height 300 mm. All specimens were based on combination of Module 1 and Module 2. Connection of specimens was applied to that of modules by arranging the general bolts in 8 mm of diameter and 25 mm of length at intervals of 200 mm. Table 1 shows the modular form and connection state of the MSC beam used in the test.

4.2 Material property

Design compressive stress of the concrete used in this test was 23.52 MPa and the concrete was cured after on-site placement. Concrete cylinder specimens made in compliance with KS F 2403 were cured under the same condition as the beams, and the compressive strength of the concrete was 25.47 MPa after testing. The test specimen of 1.6 mm in thickness was made from the SS400 cold rolled steel sheet in accordance with KS D 3503, and 2 test pieces were cut from the specimen. The strain experienced by the test pieces was measured by an attached strain gauge.

5. Experimental result

5.1 Destruction shape

5.1.1 C-type MSC beams

The destruction behavior of the C-type beam is shown in Fig. 7. Because MSC-CN did not have

Table 1 Class of specimen

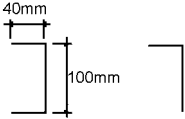
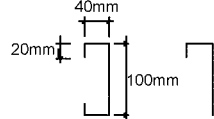
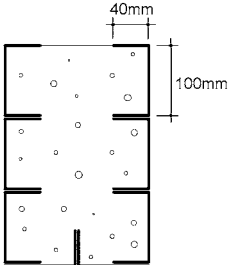
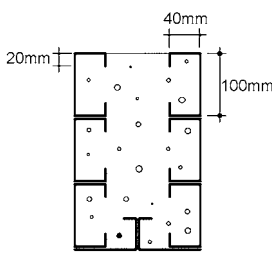
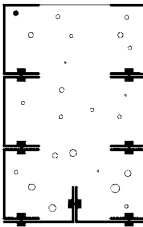
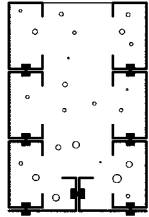
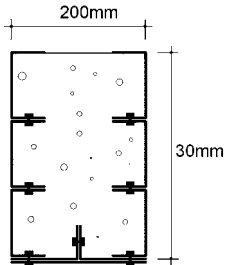
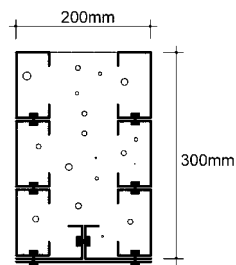
Name	Section Type	Name	Section Type
Module		Module	
MSC-CN (No Connection)		MSC-LN (No Connection)	
MSC-CB (Bolt Connection)		MSC-LB (Bolt Connection)	
MSC-CRB (Reinforced Bolt Connection)		MSC-LRB (Reinforced Bolt Connection)	

Table 2 Test result of profile

Thickness	σ_y	σ_{max}	E	Elongation ratio
1.6mm	372.4MPa	423MPa	2.04×10^5 MPa	27.4%

connection bolt between modules, slip emerged between the modules, and low stiffness and strength were measured. For MSC-CB, local buckling appeared on the module in the compression part, and lower profile steel with holes incurred from bolt connection got through the tension failure due to stress concentration. The local buckling that occurred on the module in the compression part lead to the destruction of MSC-CRB.

The specimen connected with bolts showed decrease in load after reaching maximum strength.

5.1.2 Lip-type MSC beams

The destruction shape of the L-Type beams is shown in Fig. 8. Lip-type MSC did not show plastic

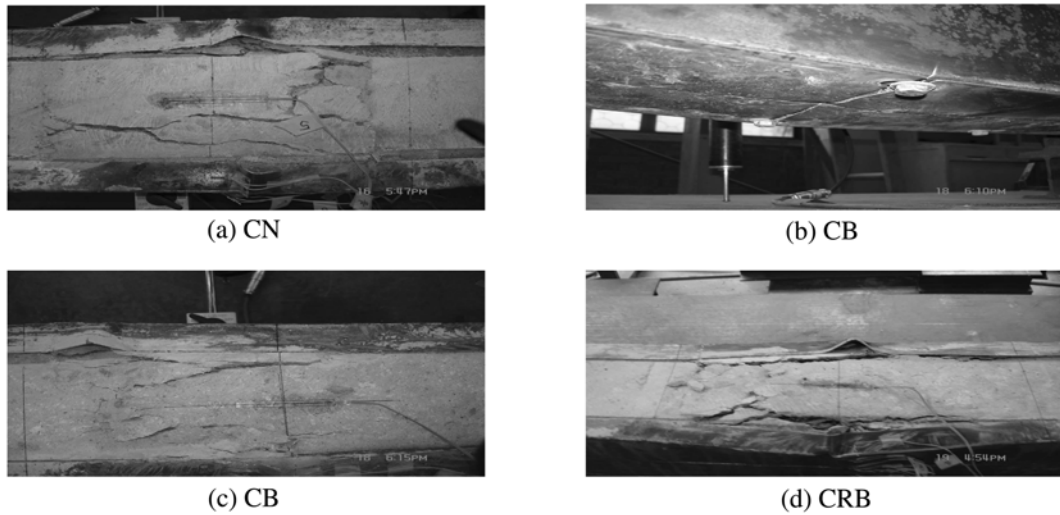


Fig. 7 Failure shape of C-type MSC beams

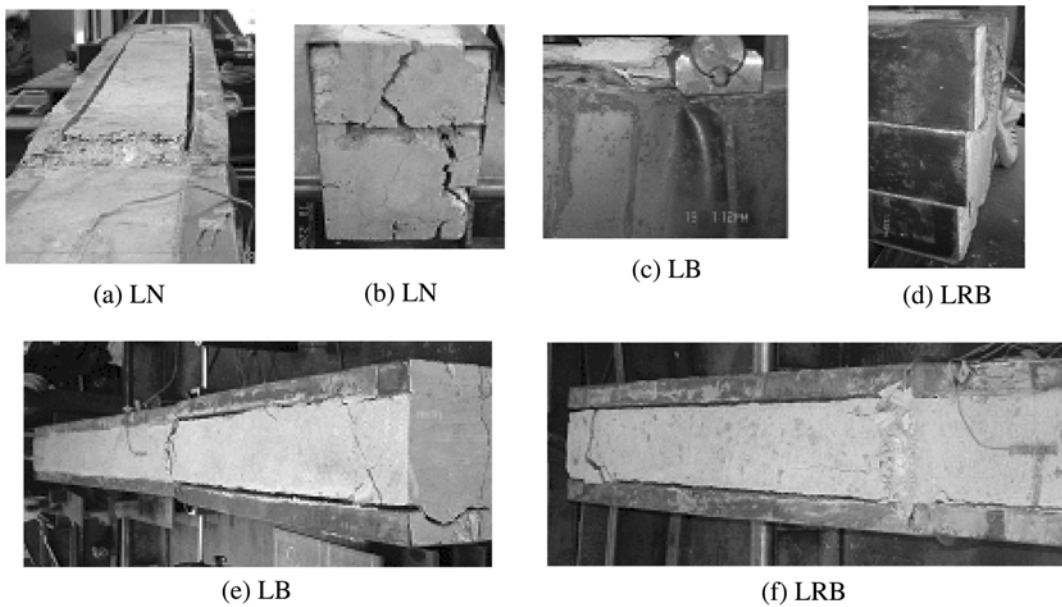


Fig. 8 Failure shape of lip-type MSC beams

behavior after reaching maximum strength but when the load was decreased, it showed deflection, which was due to the crack of the concrete in the compression part from wedge action of the Lip as well as the lateral buckling of the module in the compression part. After the load was decreased by a certain amount, a plastic behavior section was observed, because the inner concrete displayed bond strength with the remaining steel modules after lateral buckling on the upper module.

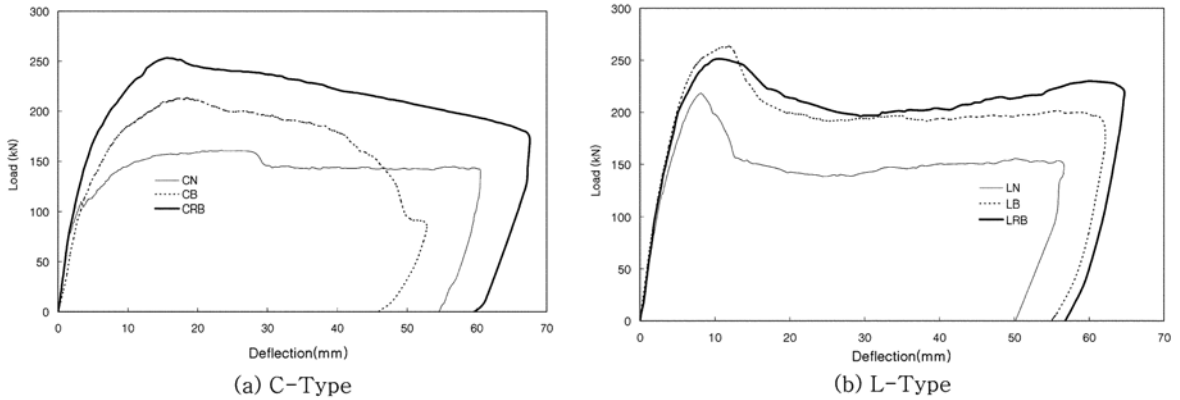


Fig. 9 Load deflection of MSC beams (midspan)

5.2 Load-deflection and load-strain curve

Fig. 9 shows the comparison among the load-deflection curves of the tested specimens. Strength varied according to type of connection of the modules in CN and CB, although they had the same amount of profile steel. Both specimens showed similar initial stiffness; however, the stiffness of the CN specimen without connection was decreased first.

CB and CRB displayed plastic behavior but did not maintain it in the plateau zone after reaching their maximum strengths. Then, load was continuously decreased. It is deemed to be due to decreased connecting force between modules. Stiffness was greater in the L-type with more steel and bonding area than C-type. However, its strength showed limited increase because of the lateral buckling of the compression module. However, such lateral buckling may be solved by the concept of the T-section beam added slab. Sharply decreased load is displayed in the L-Type after the maximum strength due to the influence of lateral buckling, and then, plastic plateau appeared after it is decreased by a certain amount.

Fig. 10 shows the load-strain curves for the upper concrete. The C-Type specimen showed full strength until collapse strain, while the L-type specimen did not reach destruction strain due to lateral buckling and did not display full strength.

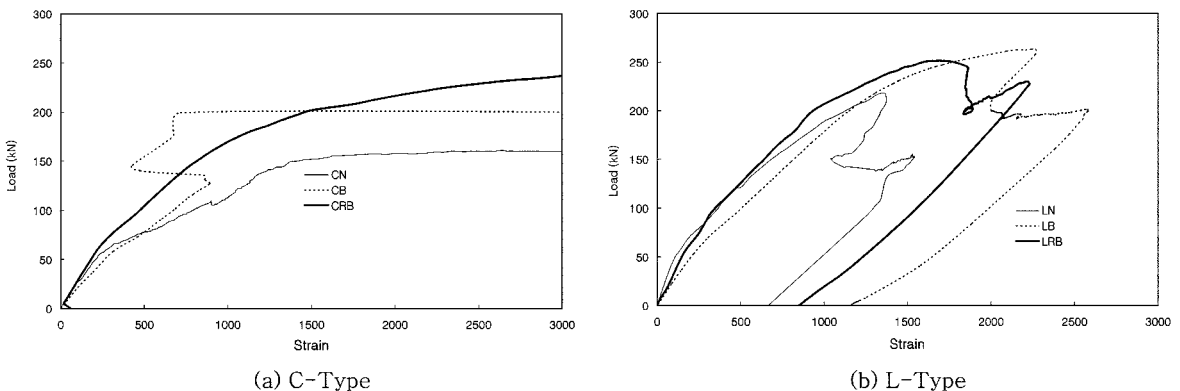


Fig. 10 Load strain of MSC beams (Top-fiber concrete strain)

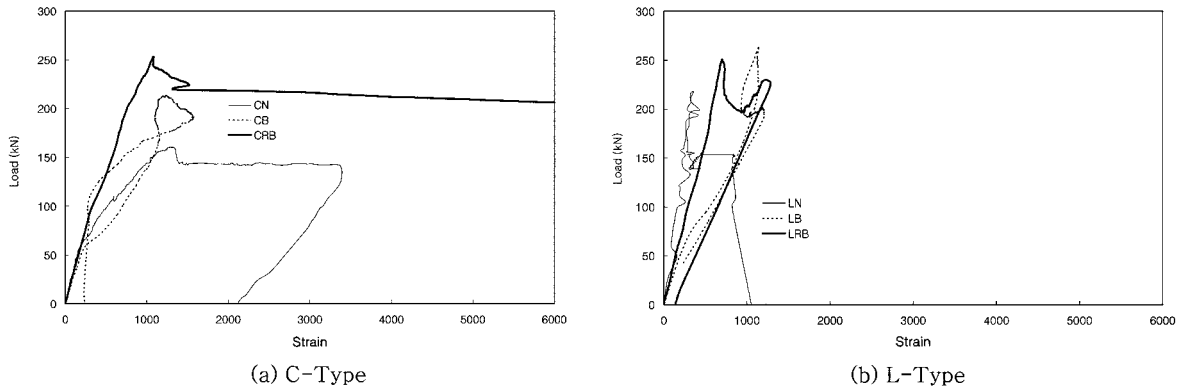


Fig. 11 Load strain of MSC beams (Bottom-fiber steel strain)

Fig. 11 shows load-strain curves for lower profile steel. CN and CB specimens displayed plastic strain in excess of yielding strain, and CRB specimen did not reach yielding but lateral buckling occurred. Lateral buckling also emerged in the L-Type specimen due to wedge action by the Lip, thus lower profile steel could not fully exercise enough strength.

5.3 Strain distribution of side profile

Fig. 12 shows the load-strain distribution of the side module. The numbers from 1 to 9 on the vertical axis indicate each location of the strain gauge (refer to Fig. 6), while the horizontal axis indicates the strain. Load is divided into 4 steps, and strain distribution is displayed according to the position of gauge per load step. Step 1 indicates the early load, step 2 40%-60% the maximum load, step 3 the maximum load, and step 4 the decreased strength after the maximum load.

The C-Type displays more strains than the L-Type. All specimens show a uniform body behavior at the beginning that the 3 modules have one neutral axis. The modules clearly separated around the maximum load in the N-series specimen without the connection of modules. Less separation between modules was shown in the B-series specimen, where the modules were connected with bolts, than in the N-series one. However, the separation became serious after what reached the maximum strength. The separation after maximum strength lead to the decreased strength of the specimen.

As for the top module of the CRB specimen, local buckling occurred at the site where a gauge was attached before the maximum load, but for the LRB specimen, the modules clearly separated after the maximum load. However, it was less than yielding stress because of the decreased strength from lateral buckling.

6. Discussion

6.1 C-type MSC beams

Theoretical and experimental maximum bending moment theories are compared in Table 3. Theoretical maximum bending moment was calculated on condition that the modules were fully

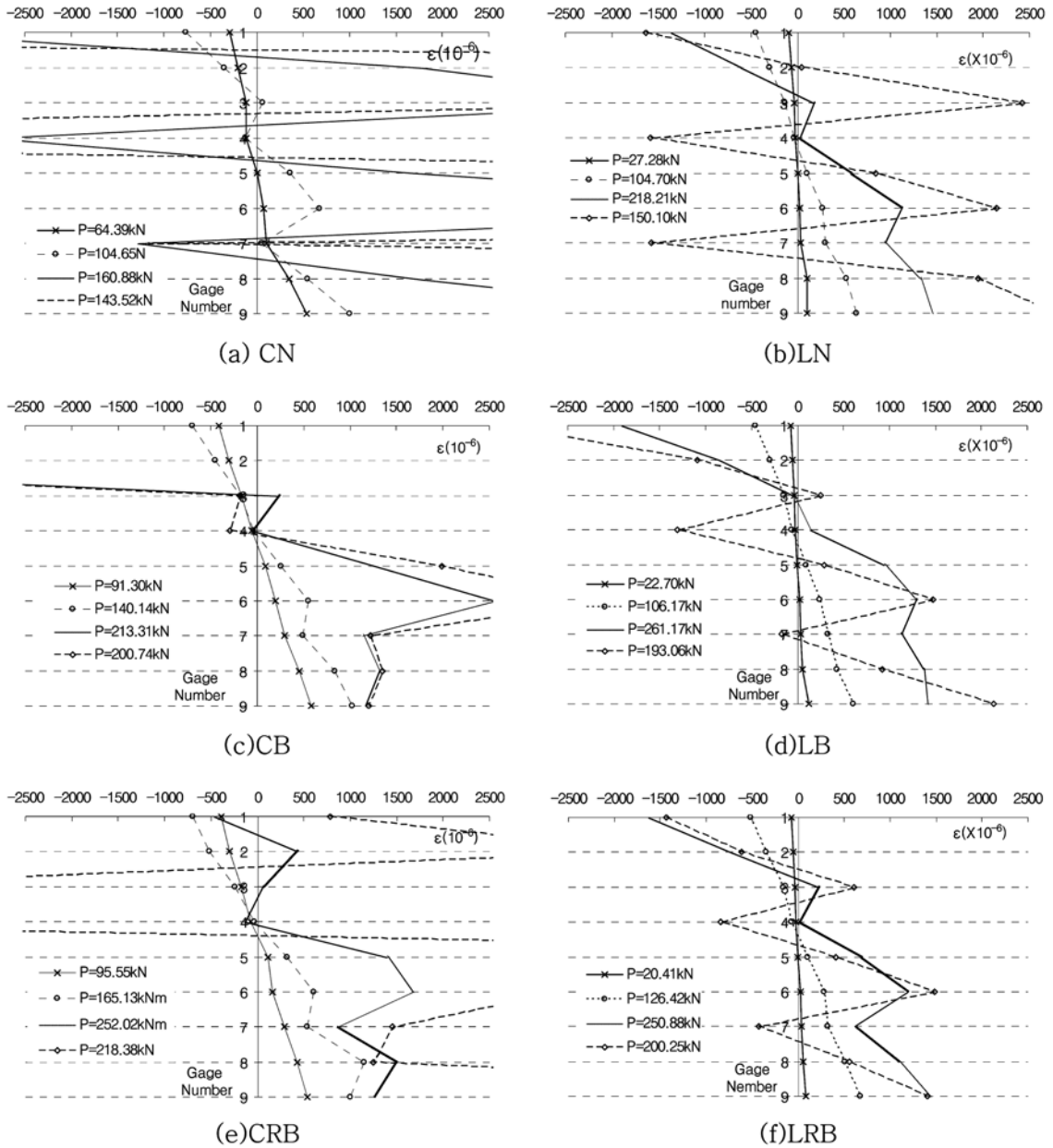


Fig. 12 Strain distribution of MSC beams according to gage number

connected and profile steel and concrete went through the full shear connection. For the CN specimen, M_{me}/M_{ml} was calculated to be 0.573 and by the theoretical method described in Paragraph 2.2, bending moment was calculated to be 112.41 kNm at full shear connection, 70.07kNm at 50% shear connection, 16.07 kNm at no shear connection. Thus, the experimental value of 64.39kNm approximated the theoretical bending moment at the 50% connection rate. Therefore, as shown by the change of the strain for the profile steel in Fig. 12(1) in Paragraph 5.3, the theory mentioned in Paragraph 2.2 was

Table 3 Maximum bending moment comparison of C-type beams

Name	M_{mt} (kNm)	M_{me} (kNm)	M_{me}/M_{mt}	a (mm)
MSC-CN	112.41	64.39	0.573	89.08
MSC-CB	112.41	85.06	0.757	89.08
MSC-CRB	125.83	101.18	0.804	94.87

M_{mt} : Theoretical maximum bending moment(Full shear connection case)

M_{me} : Experimental maximum bending moment

Table 4 Maximum bending moment comparison of L-Type beams

Name	M_{mt} (kNm)	M_{me} (kNm)	M_{me}/M_{mt}	a (mm)
MSC-LN	131.12	87.58	0.67	96.96
MSC-LB	131.12	105.37	0.80	96.96
MSC-LRB	142.59	103.21	0.72	101.71

applicable. For the MSC-BC specimen, M_{me}/M_{mt} was 0.757, and according to the equation specified in Paragraph 2.1, the bending moment was 99.27 kNm at 50% bonding and according to the equation in Paragraph 2.2, 70.07 kNm; thus, the experimental value of 85.06 kNm is between the bending moment based on Paragraph 2.1 and that based on Paragraph 2.2. By the strain distribution chart in Fig. 12(3), the strain aspect of the actual profile steel approximated the value based on Paragraph 2.2 assuming partial shear connection between modules than that based on Paragraph 2.1 assuming full connection. The bonding rate was calculated to be 70% based on Paragraph 2.2. As for the MSC-RBC specimen, M_{me}/M_{mt} was calculated to be 0.804 showing the best aspect and is deemed attributable to the incompleteness of the connection part and lateral buckling of the side sheet, as shown in Fig. 12(5). Based on the above results, the experimental results did not come up to the theoretical maximum flexural strength as fully bonded and connected however, better MSC beams can be developed through further improvement of the module connection method and inhibition of lateral buckling by introduction of the T-section beam concept.

6.2 L-type MSC beams

Theoretical and experimental maximum bending moment theories are compared in Table 4. The theoretical values of the maximum bending moment were calculated on condition that modules were fully connected and profile steel and concrete got through under full shear connection. For the MSC-NL specimen, M_{me}/M_{mt} was 0.67, and by the theoretical method described in Paragraph 2.1, bending moment was calculated to be 131.12 kNm at full shear connection, 82.81 kNm at 50% shear connection, and 19.6 kNm at no shear connection ; thus the experimental value of 87.58 kNm exceeded the theoretical value at 50% connection rate. Therefore, based on the change of the strain for the profile steel in Fig. 12(2) in Paragraph 5.3, the theory mentioned in Paragraph 2.2 was applicable. For the MSC-BC specimen, M_{me}/M_{mt} was calculated to be 0.80. According to the equation specified in Paragraph 2.1, the bending moment was 82.81 kNm at 50% shear connection and according to the equation in Paragraph 2.2, 116.62 kNm; thus, the experimental value of 105.37 kNm was between the bending moment based on Paragraph 2.1 and that based on Paragraph 2.2. From the strain distribution chart in Fig. 18, the strain of

the actual profile steel approximated the value based on Paragraph 2.2 assuming partial shear connection between modules than that based on Paragraph 2.1 assuming full connection. The composite ratio was 70% as a result of calculation following Paragraph 2.2. For the MSC-RBC specimen, M_{me}/M_{mt} was calculated to be 0.72, which indicates that the bottom reinforcing plate never contributed to the strength enhancement, and is attributable to the incompleteness of the connection part by bolt connection and lateral buckling of the side sheet under compression, as shown in Fig. 12(6). Like the C-type, a better MSC beams can be developed through further improvement of the module connection method and inhibition of lateral buckling by introduction of the concept of T-section beam.

7. Conclusions

The experimental results for MSC beams were analyzed, and flexural strength between theoretical values and experimental values was compared. Also, their behavior was analyzed according to connection between modules and reinforcement sheet under tensile strength. The following conclusions are made:

(a) All the specimens showed similar stiffness initially, but the specimens in the N showed decreased stiffness first because they had no connection between modules.

(b) After maximum strength, all specimens with connected modules showed no plastic behavior but showed decreased load due to the weakened connection part and lateral buckling. Therefore, a T-section beam must be applied and the connection part improved.

(c) Based on the theoretical values as fully connected and bonded, theoretical and experimental flexural strength ratios were 0.57 and 0.67 in the N series, 0.76 and 0.8 in the B series, and 0.76 and 0.8 in the RB series, respectively. The flexural strength ratios of B series and RB series did not reach 1.0 because of the weakened connection part and lateral buckling.

(d) In modules connected with bolts, the modules slightly separated until the maximum load was reached; however, it became serious after the maximum load. Therefore it is considered that separation between modules influences decrease in strength.

Acknowledgement

The Corresponding author was supported by the Sahmyook University Research Fund in 2006.

References

- Ahmed, M., Oehlers, D. J. and Bradford, M. A. (2000), "Retrofitting reinforced concrete beams by bolting steel plates to their sides. Part I: Behavior and experiments", *Struct. Eng. Mech., An Int. J.*, **10**(3), 211-226.
- Uy, Brian and Bradford, Andrew (1995), "Ductility of profile beams. Part 1: experimental study", *ASCE J. Struct. Eng.*, **121**(5), 876-882.
- Uy, Brian and Bradford, Andrew (1995), "Ductility of profile beams. Part I: analytical study", *ASCE J. Struct. Eng.*, **121**(5), 883-889.
- Hossain, K. M. Anwar and Wright, H. D. (2004), "Flexural and shear behavior of profiled double skin composite elements", *Steel Compo. Struct., An Int. J.*, **4**(2), 227-243.
- Peng, Minglan and Shi, Zhifei (2004), "Interface characteristics of RC beams strengthened with FRP plate", *Struct. Eng. Mech., An Int. J.*, **18**(3), 315-330.

- Oehlers, D. J. (1993), "Composite profile beams", *ASCE J. Struct. Eng.*, **119**(4), 1085-1100.
- Oehlers, D. J. Wright, H. D. and Burnet, M. J. (1994), "Flexural strength of profile beams", *ASCE J. Struct. Eng.*, **120**(2), 378-393.
- Oehlers, D. J. and Bradford, M. A. (1995), *Composite Steel and Concrete Structural Members : Fundamental Behavior*. Pergamon, UK.
- Oehlers, D. J., Ahmed, M., Nguyen, N. T. and Bradford, M. A. (1997), "Transverse and longitudinal partial interaction in composite bolted side-plated reinforced concrete beams", *Struct. Eng. Mech., An Int. J.*, **5**(5), 553-563.
- Oehlers, D. J. and Bradford, M. A. (1999), *Elementary Behavior of Composite Steel & Concrete Structural Members*, Butterworth-Heinemann, UK.
- Oehlers, D. J., Nguyen, N. T. and Bradford, M. A. (2000), "Retrofitting by adhesive bonding steel plates to sides of R.C. beams. Part 1: Debonding of plates due to flexure", *Struct. Eng. Mech., An Int. J.*, **9**(5), 491-503.
- Oehlers, D. J., Nguyen, N. T. and Bradford, M. A. (2000), "Retrofitting by adhesive bonding steel plates to sides of R.C. beams. Part 2: Debonding of plates due to shear and design rules", *Struct. Eng. Mech., An Int. J.*, **9**(5), 505-518.
- Oehlers, D. J., Ahmed, M., Nguyen, N. T. and Bradford, M. A. (2000), "Retrofitting reinforced concrete beams by bolting steel plates to their sides. Part 2: Transverse interaction and rigid plastic design", *Struct. Eng. Mech., An Int. J.*, **10**(3), 227-243.
- Kim, S. H. and Aboutaha, R. S. (2004), "Ductility of carbon fiber-reinforced polymer (CFRP) strengthened reinforced concrete beams: Experimental investigation", *Steel Compo. Struct., An Int. J.*, **4**(5).
- Smith, S. T., Bradford, M. A. and Oehlers, D. J. (1999), "Local buckling of side-plated reinforced-concrete Beams. I : Theoretical Study", *ASCE, J. Struct. Eng.*, **125**(6), 622-634.
- Smith S.T., Bradford, M. A. and Oehlers, D. J. (1999) "Local buckling of side-plated reinforced-concrete Beams. II: Experimental Study", *ASCE, J. Struct. Eng.*, **125**(6), 635-643.
- Yi Wu, He, J. and Chen, H. (2006), "Behavior of box-shape steel reinforced concrete composite beam", *Struct. Eng. Mech., An Int. J.*, **22**(4), 419-432.